

Interdependent couplings map to thermal, higher-order interactions

Ivan Bonamassa,* Bnaya Gross, and Shlomo Havlin

Department of Physics, Bar-Ilan University, 52900 Ramat-Gan, Israel

(Dated: October 19, 2021)

Interdependence is a fundamental ingredient to analyze the stability of many real-world complex systems featuring functional liasons. Yet, physical realizations of this coupling are still unknown, due to the lack of a theoretical framework for their study. To address this gap, we develop an interdependent magnetization framework and show that dependency links between $K - 1$ pairwise networks of Ising spins can be rigorously mapped to directed K -spin interactions or to adaptive thermal couplings. We adopt the thermal portrait to determine analytically the phase diagram of the model under different structural configurations and we corroborate our results by extensive simulations. We find that interdependence acts like an entropic force that amplifies site-to-site thermal fluctuations, yielding unusual forms of vulnerability and making the system's functioning often unrecoverable. Finally, we discover an isomorphism between the ground state of random multi-spin models and interdependent percolation on randomly coupled networks. This connection raises new perspectives of cross-fertilization, providing unfamiliar methods with relevant implications in the study of constraint satisfaction as well as to the functional robustness of interdependent systems.

Introduction. Paraphrasing Anderson [1], it could be said today that “more systems is different”, seeing that cross-systems interactions often yield collective phenomena that differ qualitatively from those of their isolated macro-components [2]. Interdependent systems [3] are a paradigmatic example of this thesis. Here, cross-layers couplings set mutual feedbacks between the functioning of their elements and spread perturbations across the available scales, making these adaptive systems prone to systemic risks and sudden collapses [4–10]. Despite the vast literature focusing on interdependence [11] and on its importance for catastrophic shifts in many natural [12–14] and man-made ecosystems [15–17], the *physics* underlying this interaction stands largely unexplored, lacking a theoretical benchmark to study its foundations.

In this work, we shed light on this topic by integrating interdependent interactions in the study of spin models. We show that dependency links [18] matching the nodes of $K - 1$ pairwise networks of Ising spins (Fig. 1) map to K -spin interactions on directed hypergraphs [19, 20] (Fig. 1, right) or to adaptive thermal couplings (Fig. 1, left). We analyze with extensive simulations the magnetic stability of randomly coupled Erdős-Rényi (ER) networks for arbitrary fractions of dependency links and number of layers. The model generally undergoes spontaneous first-order transitions [21–23] from a “functioning” (ferromagnetic/crystal) phase to a “malfunctioning” (paramagnetic/liquid) one from where it often fails to recover [24, 25]. In fact, we find that collapsed networks remain trapped in a “supercooled” state from where they escape only if $K = 3$ and the fraction q of interdependent spins is below a certain threshold.

We corroborate these results theoretically within the thermal portrait, where the replica-symmetric (RS) solutions [26] of the isolated networks enable to solve the

higher-order Hamiltonian via interdependent population dynamics. As a result, we find that interdependent interactions amplify the entropy production by propagating thermal fluctuations over the available scales, boosting the rate at which greedy algorithms explore the system's configurational space. This is manifested in an unusual form of extreme vulnerability [27, 28] signaled by the loss of purely marginally stable phases at low average connectivities and followed by a crossover towards the theoretical (bulk) melting spinodals [29] for increasing edge densities (concretely, graphs with $\langle k \rangle \gtrsim 10$).

Moreover, we discover an analytical mapping between the ground state (GS) of diluted ferromagnetic multi-spin models [30–32]—governing the computational complexity of random XOR-SAT [33–36], a paradigmatic problem in constraint satisfaction—and interdependent percolation on randomly coupled networks [37]. We detail this correspondence and adopt the XOR-SAT entropy [38–40] to locate the coexistence threshold delimiting the *structural metastability* of interdependent graphs. In this hitherto unknown regime—whose width, notably, diverges with the number of layers—these systems can almost surely be dismantled. However, we demonstrate with theory and simulations that percolation cascades [41, 42] remain systematically trapped in the local minima (functional states) of the free-energy landscape. Besides revealing the physical nature [43–45] of the interdependent percolation transition, this mapping raises exciting perspectives of cross-fertilization, e.g. to design optimal algorithms [46–49] for dismantling/recovering interdependent systems as well as to study networks' energy surfaces [50, 51] or ergodicity breaking [52] in real-world adaptive systems.

Interdependent spin networks. Let us consider M networks of N Ising spins $\sigma = \pm 1$ embedded in a common heat bath at temperature T . Each layer's spin configuration $\boldsymbol{\sigma} = \{\sigma_i\}_i$ has energy $-\mathcal{H}[\boldsymbol{\sigma}, A] = J \sum_{i < j} A_{ij} \sigma_i \sigma_j$, where $A = (A_{ij})_{i,j}$ is the adjacency matrix of spin-spin interactions and $J \in \mathbb{R}^+$ is their ferromagnetic strength. We model the magnetic evolution of the isolated layers

* Corresponding author: ivan.bms.2011@gmail.com
I.B. & B.G. contributed equally to this work.

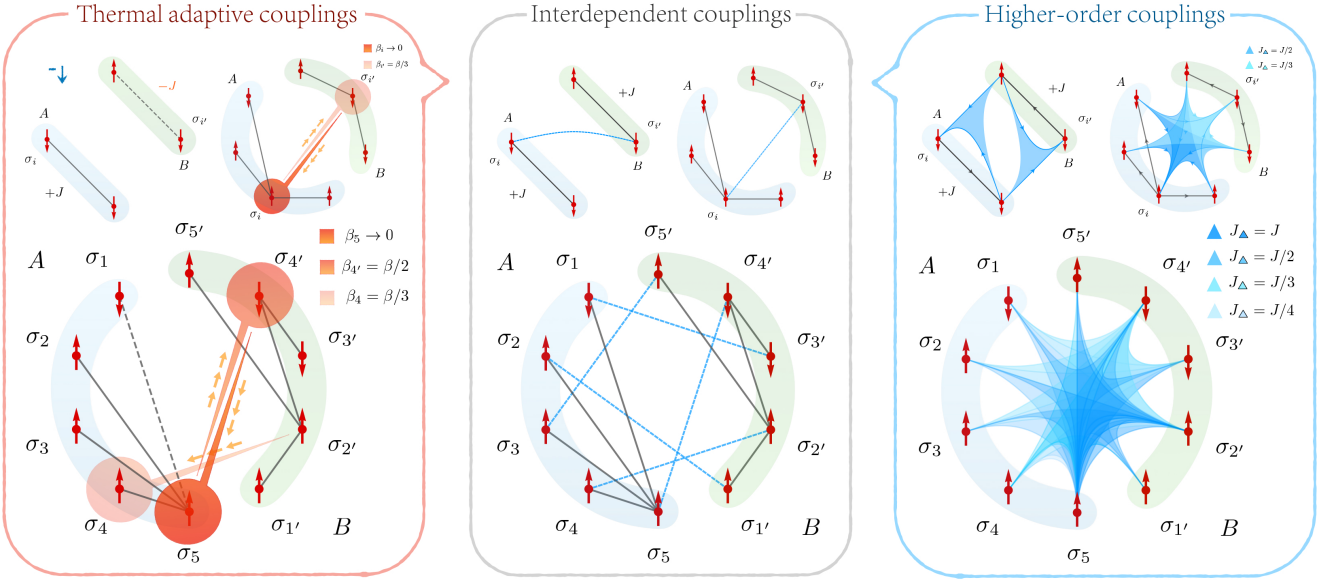


FIG. 1: **Frameworks of interdependent spin networks.** (Color online) Illustration of the physical mapping of interdependence to thermal, higher-order interactions. (Center Box) Depending on the time scales governing the system’s functioning, dependency links (dashed blue lines) between $M = 2$ networks act (see Eq. (1)) either as (Left Box) *adaptive thermal couplings*, when interdependence is slower than the layers’ thermalization, or as (Right Box) *3-spin couplings* on a directed hypergraph (notice the open hyperlinks and arrows) with Hamiltonian given by Eq. (2), when the layers’ thermalization is faster. In the thermal portrait, interdependent links generate an adaptive distribution of local temperatures (see Eq. (4)) rarely accompanied by an antiferromagnetic coupling (dashed gray bond, Left Box) due to local fields ordered in the -1 direction (blue arrow).

by means of a Glauber single spin-flip process [53]: a randomly chosen spin, σ_i , changes its sign with probability $w(\sigma_i) = (1 + e^{2\beta J k_i \sigma_i \Sigma_i})^{-1}$, where $\beta \equiv 1/T$ (in units of k_B^{-1}) and $\Sigma_i \equiv \frac{1}{k_i} \sum_j A_{ij} \sigma_j$ is the effective field created at node i by its $k_i = \sum_j A_{ij}$ neighbours. For future reference, let $\mathcal{J}_{i \leftarrow j} \equiv \beta J k_i$ be the effective coupling strength of spin i . To set interdependent interactions between layers, we adopt the Σ_i ’s as proxies for the nodes’ magnetic state [18] and intertwine their functioning via the spin-flip probabilities. Specifically, assuming e.g. that vertex i in network A depends on vertex i' in network B (Fig. 1, center box), we transform

$$\mathcal{J}_{i \leftarrow j}^A \xrightarrow{i \in A \leftarrow i' \in B} \mathcal{J}_{i \leftarrow j}^A \Sigma_{i'}^B. \quad (1)$$

In this way, σ_i gains an *adaptive coupling* [54] whose strength depends on the local order around $\sigma_{i'}$ and it flips with probability $w_i^{A \leftarrow B} = (1 + \exp\{2\mathcal{J}_{i \leftarrow j}^A \sigma_i \Sigma_{i'}^B\})^{-1}$. The role of the interdependent link is transparent: if $\sigma_{i'}$ “fails” to be functional—i.e., $\Sigma_{i'}^B \simeq 0$ —then $w_i^{A \leftarrow B} \simeq 1/2$ and σ_i fails along, since it flips sign independently of its neighbors’ order. These “concurrent malfunctions” spread across the layers over time scales to be compared with those governing their magnetization evolution. In this regard, we introduce two limiting frameworks.

◦ *Higher-order scheme* – Dependency links intertwine the magnetization kinetics of each network at the same rate of single spin-flips, making the processes’ time scales indistinguishable. An higher-order Hamiltonian $\mathcal{H}_{\mathcal{I}}$ can then be formed from those of single networks by inte-

grating Eq. (1) within the system’s structure. Let then $\mathcal{A} = A_1 \oplus \dots \oplus A_M$ be the direct sum of the networks’ matrices and $\mathcal{I} \in \mathbb{R}^{MN \times MN}$ a block matrix matching dependent nodes. For general networks of fully (see Methods for partial) interdependent Ising networks, we write

$$-\mathcal{H}_{\mathcal{I}}[\{\sigma_{\mu}\}_{\mu=1, \dots, M}, \mathcal{A}] = J \sum_{i,j} \mathcal{A}_{ij} \sigma_i \sigma_j \prod_{\ell} \mathcal{I}_{i\ell} \Sigma_{\ell}, \quad (2)$$

where $i, j, \ell = 1, \dots, MN$. If nodes of different layers are one-to-one interdependent, Eq. (2) simplifies to $-\mathcal{H}_{\mathcal{I}} = J \sum_{i_1, \dots, i_K} \mathcal{W}_{i_1 \dots i_K} \sigma_{i_1} \dots \sigma_{i_K}$, i.e. a K -spin model (with $K = M + 1$) on a hypergraph with adjacency tensor

$$\mathcal{W}_{i_1 i_2 \dots i_K} \equiv \mathcal{A}_{i_1 i_2} \prod_{\mu=1}^{M-1} \frac{\mathcal{A}_{\ell_{\mu}(i_1) i_{\mu+2}}}{k_{\ell_{\mu}(i_1)}}, \quad (3)$$

$\forall i_1 = 1, \dots, MN$, where $\{\ell_{\mu}(i_1)\}_{\mu=1, \dots, M-1}$ is the set of vertices dependent on each i_1 that belong to the remaining layers [55]. Notice that, while \mathcal{I} and \mathcal{A} are symmetric, \mathcal{W} is weighted and directed (neighboring spins depend on different nodes), generating then *incomplete* higher-order interactions (Fig. 1, right box). In this integrated portrait, sketched in Fig. 2 b for $M = 2$, the whole multilayer system evolves towards a bulk equilibrium.

◦ *Thermal scheme* – Single networks learn the equilibrium spin configuration of the layers they depend on (dependency step) and adjust theirs (magnetization step) accordingly. In this portrait [56], Eq. (1) can be physically interpreted as a thermal coupling (Fig. 1, left box)

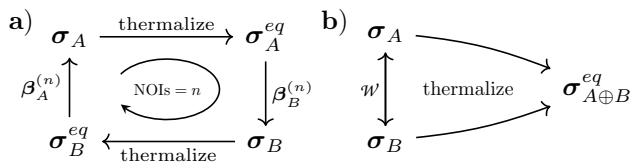


FIG. 2: **Magnetization evolution.** Diagrammatic representation of the interdependent magnetization kinetics in **a)** *slow* (thermal) and **b)** *fast* (higher-order) schemes, for $M = 2$ layers. While in the thermal framework the system equilibrates with a sequence of layer-by-layer thermalization stages, in the higher-order one the 2 networks concurrently equilibrate.

that generates a recursive sequence of local temperatures' configurations [57]. This, for e.g. 2 layers, is given by

$$\beta \xrightarrow{A \rightarrow B} \beta_B^{(1)} \xrightarrow{B \rightarrow A} \beta_A^{(1)} \xrightarrow{A \rightarrow B} \beta_B^{(2)} \dots, \quad (4)$$

where $\beta_{i,A}^{(n)} \equiv \beta \langle \Sigma_{i'}^B \rangle_{\beta_B^{(n)}}$ and $\langle (\cdot) \rangle_{\beta}$ is a thermal average. This process (Fig. 2 **a**) repeats for a number of iterations (NOIs) n , until all the layers mutually equilibrate.

Metastable functioning. Monte Carlo simulations on ER networks (Fig. 3) highly support that thermal and higher-order frameworks yield identical equilibria. Based on this equivalence, we adopt the thermal scheme to develop an analytical approach for computing thermodynamic observables of the Hamiltonian $\mathcal{H}_{\mathcal{I}}$, Eq. (2).

Slow interdependence, in fact, endows each network with a distribution β of local temperatures whose disorder is adaptively quenched by the (relative) equilibrium configurations reached by its interdependent layers. We can then resort on the replica method [26] to find the distribution of local fields $\langle \Sigma_i \rangle_{\beta}$ of each isolated network before a dependency step occurs. Based on this, we develop (see Methods for details) an *interdependent population dynamics* (iPD) algorithm to solve iteratively the sequence of local temperatures in Eq. (4). For $n \rightarrow \infty$, the distributions $\{\beta_{\mu}^{(n)}\}_{\mu=1,\dots,M}$ converge (w.h.p.) to a set of steady state configurations at which the networks' average magnetizations $\{\mathcal{M}_{\mu}^{\infty}\}_{\mu=1,\dots,M}$ become co-stable and a mutual giant magnetic component \mathcal{M} is found.

Given the iPD algorithm above, we first examine the (bulk) melting transitions [29] of $M = 2$ (Fig. 3**b**) and $M = 3$ (Fig. 3**a**) randomly *fully*-coupled ER Ising networks with equal average degree $\langle k \rangle$. Theoretical thresholds coincide (within numerical accuracy) with the RS-ones featured by ferromagnetic $(M + 1)$ -spin models on random hypergraphs [32] with average hyperdegree $\langle k \rangle$ (dotted curves, Fig. 3**a,b**). Notably, both models host ferromagnetic spinodals [21] above structural thresholds $\langle k \rangle_{sp}$ (dot-dashed lines, Fig. 3**a,b**) matching the tipping points of percolation cascades [6] in fully-coupled ER networks. We explore this surprising connection in the upcoming section. Let us focus now on the agreement of the above with Monte Carlo simulations.

Full symbols in Fig. 3**a,b** show that simulations on ER graphs with $\langle k \rangle \gtrsim 10$ fit nicely the analytical predictions, while sparser structures are extremely more fragile. The

theoretical equivalence with hypergraphs suggests that this stronger low- $\langle k \rangle$ vulnerability stems from a systemic amplification of thermal fluctuations by interdependence. Diluted multi-spin models, in fact, undergo two relevant ground state (GS) transitions [31, 32]: a *dynamical* (clustering) one, precisely at $\langle k \rangle_{sp}$, where marginally stable ferromagnetic solutions appear [38–40], followed by a *static* one at $\langle k \rangle_{cx}$ (double-dot-dashed lines, Fig. 3**a,b**), where the ferro-para transition takes place. Greedy algorithms generally remain trapped in the local energy minima between these thresholds [36], resulting in (exponentially) long-lived metastable functional states [21]. Interdependent interactions, on the other hand, randomly spread the thermal fluctuations of the fields Σ_i , acting as infinite-range entropic forces that randomize the kinetics of local Glauber-like algorithms. This phenomenon boosts the phase-space exploration [58], yielding the loss of the purely metastable phases between $\langle k \rangle_{sp}$ and $\langle k \rangle_{cx}$, followed by a crossover to the expected spinodals as the fluctuations weaken. To verify the above scenario, we notice that iPD algorithms root on a thermal averaging, so they are blind to site-to-site thermal fluctuations. This motivates two distinct experiments: *i*) setting global (all-to-one) interdependence by replacing Σ_i^{μ} in Eq. (1) with the global magnetizations $\mathcal{M}_{\mu}^{\infty}$, so that thermal fluctuations are surely negligible; *ii*) planting synthetic Gaussian fluctuations as $\Sigma_i^{\mu} + \xi_i$, with $\xi_i \in \mathcal{N}(0, a/\langle k \rangle)$, whose strength decreases with $\langle k \rangle$. The resulting analytical behaviors, depicted in Fig. 3**a,b** with *i*) dot-dashed and *ii*) dashed curves, show excellent agreement with numerical simulations (open symbols) and corroborate in two independent ways the thermal fluctuations' scenario.

Another relevant aspect emerges when attempting to revive failed states. Large-scale collapses turn out to be *irreversible* in fully-coupled networks, with systems staying unmagnetized even when quenched down to near-zero temperatures. The hypergraph equivalence comes again in hand, associating the lack of spontaneous recovery to a *supercooling* process, during which the system's evolution becomes insensitive to the functional GS. However, if hypergraphs undergo a glass transition [31, 32] at temperatures accessible by simulated annealing (Fig. 3**b**, inset), interdependent spin networks do not, due to their high hyperedge density, $\gamma = \langle k \rangle^M$ (see Methods).

The case of partial interdependence is summarized in Fig. 3**c,d** for $\langle k \rangle = 4$. We find that the melting spinodals (full curve) follow here only qualitatively the RS-ones of diluted $(2 + q)$ - and $(3 + q)$ -spin models for $q \in (0, 1)$ [39], with small deviations (Fig. 3**c**, inset) whose sign reverses as $\langle k \rangle$ increases. Alike the $q = 1$ case, local thermal fluctuations erode the functional metastability—as we verify in Fig. 3**c,d** via iPD endowed with synthetic noise (dashed curve) and with global interdependence (dot-dashed curve)—and “supercooled” failed phases set in for any $M > 2$ and any fraction q of cross-couplings. Spontaneous recovery takes place only in $M = 2$ weakly coupled graphs. Numerical thresholds reported in Fig. 3**c,d** by crosses (noisy iPD) and points (global iPD), reveal

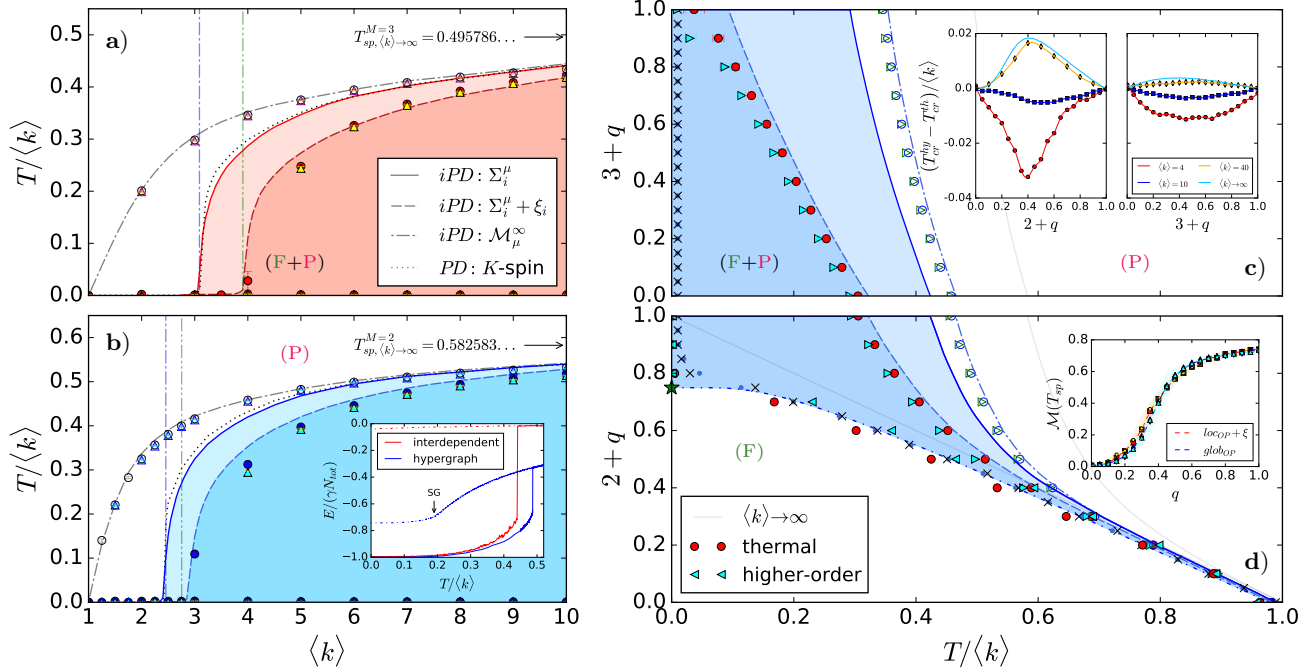


FIG. 3: Extreme vulnerability and non-recoverability. (Color online) Analytical (iPD) and numerical (Monte Carlo) phase diagrams for interdependent magnetization in (left column) fully-coupled and (right column) partially-coupled ER networks of Ising spins with (bottom row) $M = 2$ and (top row) $M = 3$ layers. Colored phases correspond to areas of functional (ferro-para) metastability. **(a, b)** Melting spinodals obtained via the iPD in Eq. (11) (full curves), noisy iPD with variances $a_{M=2} = 1.22$ and $a_{M=3} = 1.55$ (dashed curves), iPD with global OP couplings (dot-dashed curve), and standard PD for a diluted $(M + 1)$ -spin model (dotted curve). Thresholds are averaged over 100 runs with networked populations of size $N = 10^4$ and convergence is found after $T = 10^3 - 10^4$ iterations. The dot-dashed (double-dot-dashed) line marks the hyperbackbone [hyperloop] percolation threshold $\langle k \rangle_{sp} = 2.4554(1)$ [$\langle k \rangle_{cx} = 2.7538(0)$] for $M = 2$ and $\langle k \rangle_{sp} = 3.0891(1)$ [$\langle k \rangle_{cx} = 3.9870(8)$] for $M = 3$. For $\langle k \rangle \gtrsim 10^2$, the iPD thresholds converge to $T_{sp, \langle k \rangle \rightarrow \infty}(M)$ calculated within the annealed network approximation (see Methods). **(b)** (Inset) 3-spin energy density as in Eq. (2) for $M = 2$ fully interdependent ER graphs with $\langle k \rangle = 6$ and for a random hypergraph with edge density $\gamma = 2$. Notice that $\gamma = \langle k \rangle / 3$ and $N_{tot} = N$ for hypergraphs while $\gamma = \langle k \rangle^2$ and $N_{tot} = 2N$ in interdependent graphs. **(c, d)** Results of iPD for $M = 2$ (bottom) and $M = 3$ (top) ER graphs with $\langle k \rangle = 4$ and partial $q \in [0, 1]$ couplings; in noisy iPD, we adopted the variances $a_{2+q} = 1.22q$ and $a_{3+q} = (1.22 + q/3)$. In $2 + q$ layers, functional recovery (i.e. a para-ferro transitions at finite T) occurs only below $q' = 3/4$ (star symbol) with tricritical point $q_c \rightarrow 0^+$, while in $3 + q$ layers the loss of functionality is irreversible for any $q \in [0, 1]$. **(d)** (Inset) Critical magnetizations $\mathcal{M}(T_{sp})$ versus q for global and noisy iPDs. **(c)** (Inset) Difference between the melting spinodals of interdependent spin networks and of ferromagnetic $(M + q)$ -spin models on random hypergraphs at finite connectivities (see SI for details). Notice the inversion taking place around $\langle k \rangle = 10$. *Simulations.* Circles display the results (averages taken over 500 runs) of simulations in the thermal scheme (Fig. 2a) on synthetic ER graphs of size $N = 10^5$ after $MCSs = 10^5 \times N$ Monte Carlo steps and $NOIs = 10^2$ dependency iterations. Similarly, triangles depict the thresholds calculated in the higher-order scheme (see Fig. 2b) with $N_{tot} = 2N$ and $MCSs = 10^5 \times N \times NOIs$.

that para-ferro transitions occur at finite T only below $q' = 1 - 1/\langle k \rangle$ (Fig. 3d, green star). In fact, the whole line $(q_{tc}, T_{tc}/\langle k \rangle)$ of para-ferro transitions can be characterized analytically as $\langle k \rangle(1 - q_{tc})\tanh(\beta_{tc}) = 1$, identifying the line of transcritical bifurcations governed by the fraction $(1 - q)$ of independent/pairwise-coupled spins in both the interdependent and the $(2 + q)$ -spin models (see SI). This equivalence further enables to locate the tricritical point, q_c , in the $(q, T/\langle k \rangle)$ phase plane. We find that $q_c \rightarrow 0^+$, i.e. interdependent spin networks undergo first-order transitions for *any* finite fraction of cross-layers couplings, as verified via iPD (Fig. 3d, inset). Similarly to interdependent percolation in randomly coupled 2D-lattices [27], this acute fragility can be explained in light of the Ising mean-field universality class in ER

graphs, characterized by an exponent $\beta = 1/2 < 1$.

Interdependence meets XOR-SAT. Figs. 3a,b show that the RS-GS of fully interdependent spin networks at $T = 0$ coincides numerically with the critical connectivity, $\langle k \rangle_{sp}$, of cascading failures in their percolation analogue [6, 7]. At the very same threshold, diluted K -spin models with $K \equiv M + 1$ (dotted curves, Fig. 3a,b)—and, more generally, $(M + q)$ -spin models [39]—undergo a dynamic transition marking the percolation of the 2-core in the underlying hypergraph [40]. We find that this surprising correspondence stems, in fact, from an analytical mapping between the models. At $T = 0$, the RS-magnetization m (i.e., the hyperbackbone) of the K -spin model equals the largest root of $m = 1 - \exp\{-\langle k \rangle m^{K-1}\}$, which is precisely the branching order parameter (OP)—called $1 - f$ in Refs. [6, 7]—of interdependent percolation in M fully-

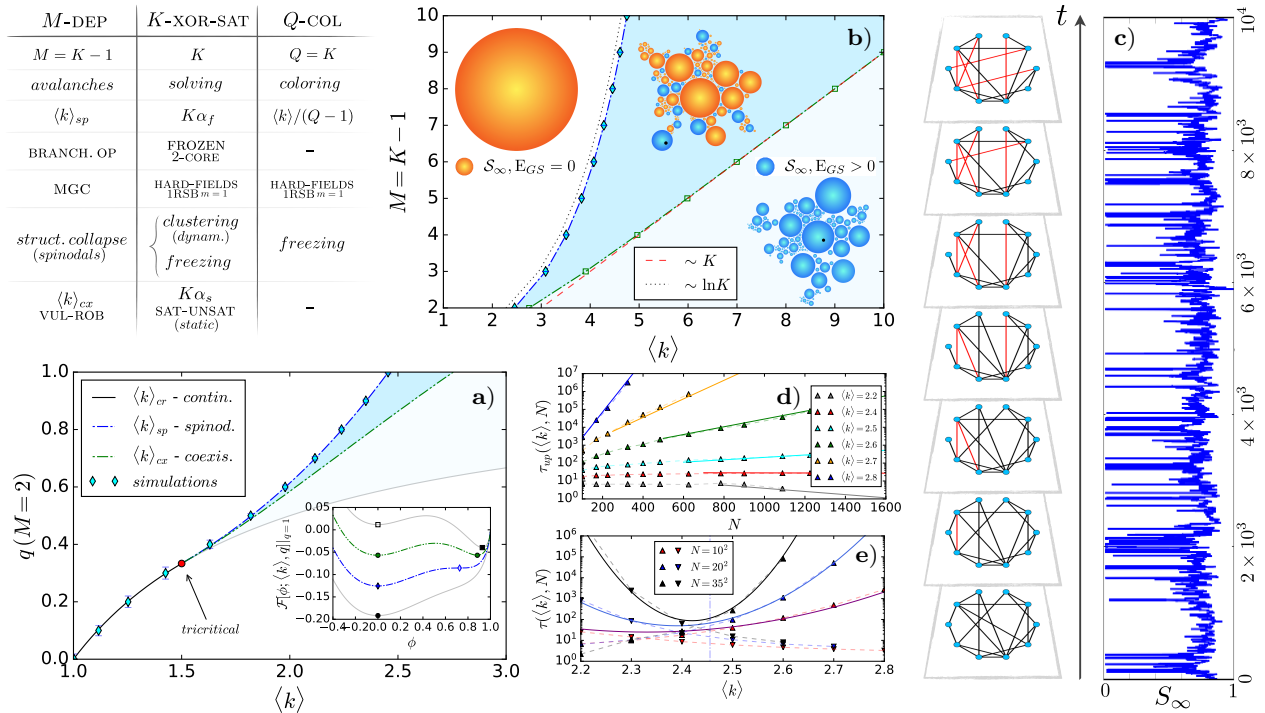


FIG. 4: **Structural metastability of interdependent networks.** (Color online) Colored phases portrait areas of metastability. **a)** Phase diagram of $M = 2$ partially-coupled ER networks displaying the analytical spinodals (dot-dashed curve) and the VUL-ROB coexistence (double-dot-dashed curve). Notice the finite tricritical point $(q_c, \langle k \rangle_c) = (3/2, 1/3)$ and the formal line of transcritical bifurcations (full grey curve). (Inset) RS-free energy density, Eq. (5), for $q = 1$ and $\langle k \rangle = 2.17, 2.46, 2.75, 3.05$ (from bottom to top), indicating stable (full symbols) and marginally stable (empty symbols) states. **b)** Extension of the above to $M \geq 2$ fully-coupled ER graphs [values of $\langle k \rangle_{cx}(M)$ are obtained from Eq. (14) in Methods]; notice the linear growth of the VUL-ROB thresholds (dashed curve) versus the logarithmic one of the spinodals (dotted curve). (Inset) Sketch of the configurational space of cascading failures (see text for its description); notice the planted UNSAT configuration (black dot). **c)** Evolution of the MGC, \mathcal{S}_∞ , for $M = 2$ small ($N = 10^2$) fully-coupled temporal ER graphs at $\langle k \rangle = 2.6$ undergoing a random rewiring of single links at each time step; single runs are obtained by regenerating the cascading process. **d)** Finite-size scaling of the MGC's average lifetime τ in the alive (connected) phase for varying $\langle k \rangle$. Critical slowing down is marked by the sub-exponential scaling at $\langle k \rangle = 2.4 - 2.5$; full lines correspond to the first-passage time estimate in the text. **e)** Scaling of τ versus $\langle k \rangle$ for given N ; as predicted by the first-passage time estimate, an exponential inversion between the alive and collapsed phases occurs precisely at the structural spinodal $\langle k \rangle_{sp} = 2.455(1)$ (dot-dashed line). *Table.* Connections among interdependent percolation on M randomly coupled ER networks (M -DEP), random K -XOR-SAT [45] and random Q -Coloring [44]. *Simulations.* Symbols in **(a,b)** show the thresholds (averaged over 10^3 runs) of simulated cascading failures on ER graphs with $N = 10^5 - 10^6$.

coupled ER graphs. An analogous mapping is found also in the case of partial couplings (see Methods). Thanks to this connection, the RS-GS entropy of multi-spin models becomes a proxy for the free energy, \mathcal{F} , of interdependent networks, enabling to delimit their *structural metastability*. E.g., for two partially coupled ER graphs

$$-\mathcal{F}[\phi; \langle k \rangle, q] / \ln 2 = \phi - \frac{1}{2} \langle k \rangle (1 + q) \phi^2 + \frac{2}{3} \langle k \rangle q \phi^3, \quad (5)$$

s.t. $\phi = \exp\{-\langle k \rangle(1 - \phi)(1 - q\phi)\}$ [39]; a general formula for M layers is given in the Methods. The landscape of \mathcal{F} (Fig. 4a, inset) unfolds the coexistence threshold, $\langle k \rangle_{cx}$ (Figs. 4a,b), where hyperloops (frustration) percolate in hypergraphs [40] and interdependent networks transition from vulnerable (VUL) to robust (ROB) structures.

A relevant implication of the above is that, in randomly interdependent ER graphs, the metastability width grows linearly with the number of layers. One finds [43–45] that $\langle k \rangle_{sp} = \ln K + \mathcal{O}(\ln \ln K)$ (Fig. 4b, dotted curve) while

$\langle k \rangle_{cx} \sim K$ (Fig. 4b, dashed curve) for $K \gg 1$, unveiling that typical instances of networks of ER graphs can almost surely be dismantled over regimes of connectivity much broader than those found in previous studies [37].

The comparison against simulated cascading failures raises, nevertheless, some intriguing puzzles. We find that typical runs on large ER graphs (Fig. 4a,b, filled symbols) are completely insensitive to the paramagnetic GS, remaining mutually connected even when quenched much below the VUL-ROB threshold. Hallmarks of criticality appear only in the vicinity of the spinodals $\langle k \rangle_{sp}$, where local cascades yield extensive avalanches. This is nicely confirmed by simulations on two fully-coupled temporal ER networks of increasing size, N , whose structure evolves by randomly rewiring single links at each time step (Fig. 4c). In this case, the average lifetime τ_{up} of the system in the alive ($\mathcal{S}_\infty > 0$) phase—defined by the relative size, \mathcal{S}_∞ , of the mutual giant component (MGC)—marks the onset of criticality at $\langle k \rangle_{sp} = 2.4554(1)$, dis-

playing critical slowing down therein (Fig. 4d) and an exponential growth (decay) with N above (below) it. Similar results arise from the scaling of τ with $\langle k \rangle$ at fixed N (Fig. 4e), further supported by the first-passage time [59] estimate $\tau \sim \sqrt{N} \exp\{\kappa N (\langle k \rangle - \langle k \rangle_{sp}(N))^2\}$. Why then interdependent networks do not fragment below $\langle k \rangle_{cx}$? Most curiously, why cascading failures reach the spinodals [60, 61], seeing that these singularities are notoriously inaccessible due to the instability of systems deep quenched in their metastable regime [62–64]?

Both puzzles can be resolved by an isomorphism between interdependent percolation and XOR-SAT, a prominent constraint satisfaction problem (CSP) [36]. Solutions to random K -XOR-SAT (see Methods) are in one-to-one correspondence [33–35] with the $T = 0$ GSs of diluted K -spin models and, as such, they exist for any density, α , of combinatorial constraints (clauses) smaller than the SAT-UNSAT threshold $\alpha_s \equiv \langle k \rangle_{cx}/K$, where hyperloops percolate [38–40]. The computational cost of finding solutions, however, undergoes an abrupt easy-hard transition at the so-called *freezing* threshold $\alpha_f < \alpha_s$ [43–45], marking the onset of complexity in local algorithms. The OP, ψ , of the K -XOR-SAT freezing transition—called $1-t$ in Ref. [40]—measures the fraction of hard cavity fields in the 1RSB solution with Parisi parameter $m = 1$ [45] and satisfies the self-consistent equation

$$\psi = (1 - e^{-K\alpha\psi})^{K-1}, \quad (6)$$

which also defines the MGC of interdependent percolation in $K - 1$ fully-coupled ER graphs with $\langle k \rangle \equiv K\alpha$ [37]. We stress that Eq. (6) governs also the freezing in random Q -COLORING [65] (see Table in Fig. 4).

This bijection makes $\langle k \rangle_{sp}$ the threshold locating [66] the spontaneous (ergodicity) breaking of GSs into an exponential number of clusters (Fig. 4b, orange disks), accompanied by the proliferation of metastable states with positive energy (Fig. 4b, blue disks). A connection can then be put forward: interdependent ER graphs collapse whenever cascading failures find a XOR-SAT solution. In this portrait, percolation cascades attempt at solving random K -XOR-SAT by adaptively modifying the variables of $K - 1$ planted configurations (Fig. 4b, black dots), sampled from the UNSAT phase of a random 2-XOR-SAT (i.e. connected ER graphs) with the same density of constraints. Interdependent links constrain then the boolean variables (functioning states) of different 2-XOR-SAT “layers” by setting a logical AND between them.

We arrive to an answer for both the above conundra. Below $\langle k \rangle_{sp}$, planted UNSAT configurations are *quiet* [65], since metastable states are absent and the failed (liquid) phase remains a stable fixed point of the cascading pro-

cess. Above $\langle k \rangle_{sp}$, instead, planting irreversibly biases the avalanches towards one of the many metastable (functional) states. Clusters of XOR-SAT solutions remain, thus, always hidden from percolation cascades so that giant avalanches never occur below the coexistence connectivity $\langle k \rangle_{cx}$. The structural spinodal $\langle k \rangle_{sp}$ can then be reached, emerging as the only critical singularity of the process. This is reminiscent of quiet planting in random graph coloring [65] and suggests that interdependent percolation may be adopted as an unconventional whitening protocol [67] for random satisfiability problems.

Discussion. Connections between disciplines are often powerful sources of new understanding [68]. The realization of interdependence as a thermal, higher-order interaction has led us to unveil some deep insights and useful links among the theory of interdependent systems, spin glasses and CSPs, raising unfamiliar perspectives on traditional problems and opportunities of cross-fertilization. For instance, mapping cascading failures of interdependent networks to XOR-SAT solutions generates fertile grounds to design efficient algorithms that apply computational complexity methods for the optimal functioning of adaptive complex systems. Their applicability, in this respect, would be broad and interdisciplinary, providing fresh viewpoints for e.g. controlling systemic risks and collapses in real-world ecosystems [10, 69], solving AI or cryptography problems [70], studying transient chaos [71] and more. From a theoretical viewpoint, the equivalence of Eq. (6) with the MGC of interdependent percolation on randomly coupled ER graphs brings an unorthodox testbed to study the universal features of the RSB mechanisms (e.g. hard-field distributions, clustering, point-to-set correlations, tree reconstruction [72], *etc.*). This perspective becomes even richer if we consider that the thermal realization of interdependence raises an unprecedented opportunity for their experimental realization in e.g. thermally coupled electrical arrays, where local Joule heating can embody the spontaneous set in of dependency links. In granular ferromagnets [73], e.g., electrons hopping from grain to grain (i.e. Ising spins) experience strong scattering (high resistance) if the neighboring grains are magnetically disordered (i.e. $\Sigma_i \simeq 0$) producing, as in Eq. (1), a local increase in the temperature of the superposed grain that can promote its probability to become disordered w.r.t. its own neighbors. To this aim, the extension of the present analysis to other topologies (e.g. spatial networks) is desirable and we expect that connections similar to those we have detailed here in random structures will be found, raising the potential to unveil other elegant connections.

-
- [1] P. W. Anderson. More is different. *Science*, 177(4047):393–396, 1972.
 [2] Eva Y Andrei, Dmitri K Efetov, Pablo Jarillo-Herrero,

- Allan H MacDonald, Kin Fai Mak, T Senthil, Emanuel Tutuc, Ali Yazdani, and Andrea F Young. The marvels of moiré materials. *Nature Reviews Materials*, pages 1–6,

- 2021.
- [3] S.M. Rinaldi, J.P. Peerenboom, and T.K. Kelly. Identifying, understanding, and analyzing critical infrastructure interdependencies. *Control Systems, IEEE*, 21(6):11–25, 2001.
 - [4] Simon A Levin. Ecosystems and the biosphere as complex adaptive systems. *Ecosystems*, 1(5):431–436, 1998.
 - [5] Marten Scheffer. *Critical transitions in nature and society*, volume 16. Princeton University Press, 2009.
 - [6] Sergey V. Buldyrev, Roni Parshani, Gerald Paul, H. Eugene Stanley, and Shlomo Havlin. Catastrophic cascade of failures in interdependent networks. *Nature*, 464(7291):1025–1028, Apr 2010.
 - [7] Roni Parshani, Sergey V. Buldyrev, and Shlomo Havlin. Interdependent Networks: Reducing the Coupling Strength Leads to a Change from a First to Second Order Percolation Transition. *Phys. Rev. Lett.*, 105:048701, Jul 2010.
 - [8] Per Hokstad, Ingrid B Utne, and Jørn Vatn. *Risk and interdependencies in critical infrastructures*. Springer, 2012.
 - [9] Dirk Helbing. Globally networked risks and how to respond. *Nature*, 497(7447):51–59, 2013.
 - [10] Mauro F Guillén. *The architecture of collapse: The global system in the 21st century*. Oxford University Press, USA, 2015.
 - [11] Ginestra Bianconi. *Multilayer Networks: Structure and Function*. Oxford University Press, 2018.
 - [12] Michael JO Pocock, Darren M Evans, and Jane Memmott. The robustness and restoration of a network of ecological networks. *Science*, 335(6071):973–977, 2012.
 - [13] Alex Fornito, Andrew Zalesky, and Michael Breakspear. The connectomics of brain disorders. *Nature Reviews Neuroscience*, 16(3):159–172, 2015.
 - [14] David F Klosik, Anne Grimbs, Stefan Bornholdt, and Marc-Thorsten Hütt. The interdependent network of gene regulation and metabolism is robust where it needs to be. *Nature communications*, 8(1):534, 2017.
 - [15] Andrew G Haldane and Robert M May. Systemic risk in banking ecosystems. *Nature*, 469(7330):351, 2011.
 - [16] Giuliano Andrea Pagani and Marco Aiello. The power grid as a complex network: a survey. *Physica A: Statistical Mechanics and its Applications*, 392(11):2688–2700, 2013.
 - [17] Juan C Rocha, Garry Peterson, Örjan Bodin, and Simon Levin. Cascading regime shifts within and across scales. *Science*, 362(6421):1379–1383, 2018.
 - [18] Michael M Danziger, Ivan Bonamassa, Stefano Boccaletti, and Shlomo Havlin. Dynamic interdependence and competition in multilayer networks. *Nature Physics*, 15(2):178, 2019.
 - [19] Federico Battiston, Giulia Cencetti, Iacopo Iacopini, Vito Latora, Maxime Lucas, Alice Patania, Jean-Gabriel Young, and Giovanni Petri. Networks beyond pairwise interactions: structure and dynamics. *Physics Reports*, 2020.
 - [20] F BATTISTON, E Amico, A Barrat, G Bianconi, GF de Arruda, B Franceschiello, I Iacopini, S Kefi, V Latora, Y Moreno, et al. The physics of higher-order interactions in complex systems. *Nature Physics*, 2021.
 - [21] Kurt Binder. Theory of first-order phase transitions. *Reports on progress in physics*, 50(7):783, 1987.
 - [22] Theodore R Kirkpatrick and Devarajan Thirumalai. p-spin-interaction spin-glass models: Connections with the structural glass problem. *Physical Review B*, 36(10):5388, 1987.
 - [23] Giulio Biroli and Jean-Philippe Bouchaud. The random first-order transition theory of glasses: a critical assessment. *Structural Glasses and Supercooled Liquids: Theory, Experiment, and Applications*, pages 31–113, 2012.
 - [24] Antonio Majdandzic, Boris Podobnik, Sergey V. Buldyrev, Dror Y. Kenett, Shlomo Havlin, and H. Eugene Stanley. Spontaneous recovery in dynamical networks. *Nature Physics*, 10(1):34–38, Dec 2013.
 - [25] Hillel Sanhedrai, Jianxi Gao, Moshe Schwartz, Shlomo Havlin, and Baruch Barzel. Reviving a failed network via microscopic interventions. *arXiv preprint arXiv:2011.14919*, 2020.
 - [26] Marc Mézard, Giorgio Parisi, and Miguel Virasoro. *Spin glass theory and beyond: An Introduction to the Replica Method and Its Applications*, volume 9. World Scientific Publishing Company, 1987.
 - [27] Amir Bashan, Yehiel Berezin, Sergey V. Buldyrev, and Shlomo Havlin. The extreme vulnerability of interdependent spatially embedded networks. *Nature Physics*, 9:667–672, Aug 2013.
 - [28] Michael M Danziger, Louis M Shekhtman, Amir Bashan, Yehiel Berezin, and Shlomo Havlin. Vulnerability of interdependent networks and networks of networks. In *Interconnected Networks*, pages 79–99. Springer, 2016.
 - [29] Florent Krzakala and Lenka Zdeborová. On melting dynamics and the glass transition. i. glassy aspects of melting dynamics. *The Journal of chemical physics*, 134(3):034512, 2011.
 - [30] Bernard Derrida. Random-energy model: Limit of a family of disordered models. *Physical Review Letters*, 45(2):79, 1980.
 - [31] Federico Ricci-Tersenghi, Martin Weigt, and Riccardo Zecchina. Simplest random k-satisfiability problem. *Physical Review E*, 63(2):026702, 2001.
 - [32] Silvio Franz, Marc Mézard, Federico Ricci-Tersenghi, Martin Weigt, and Riccardo Zecchina. A ferromagnet with a glass transition. *EPL (Europhysics Letters)*, 45(4):465, 2001.
 - [33] Scott Kirkpatrick, C Daniel Gelatt, and Mario P Vecchi. Optimization by simulated annealing. *science*, 220(4598):671–680, 1983.
 - [34] Rémi Monasson, Riccardo Zecchina, Scott Kirkpatrick, Bart Selman, and Lidror Troyansky. Determining computational complexity from characteristic “phase transitions”. *Nature*, 400(6740):133–137, 1999.
 - [35] Marc Mézard, Giorgio Parisi, and Riccardo Zecchina. Analytic and algorithmic solution of random satisfiability problems. *Science*, 297(5582):812–815, 2002.
 - [36] Marc Mezard and Andrea Montanari. *Information, physics, and computation*. Oxford University Press, 2009.
 - [37] Jianxi Gao, Sergey V. Buldyrev, H. Eugene Stanley, and Shlomo Havlin. Networks formed from interdependent networks. *Nature Physics*, 8(1):40–48, 2012.
 - [38] Silvio Franz, Michele Leone, Federico Ricci-Tersenghi, and Riccardo Zecchina. Exact solutions for diluted spin glasses and optimization problems. *Physical Review Letters*, 87(12):127209, 2001.
 - [39] Michele Leone, Federico Ricci-Tersenghi, and Riccardo Zecchina. Phase coexistence and finite-size scaling in random combinatorial problems. *Journal of Physics A: Mathematical and General*, 34(22):4615, 2001.
 - [40] Marc Mézard, Federico Ricci-Tersenghi, and Riccardo

- Zecchina. Two solutions to diluted p-spin models and xorsat problems. *Journal of Statistical Physics*, 111(3-4):505–533, 2003.
- [41] Christian M Schneider, Nuno AM Araújo, and Hans J Herrmann. Algorithm to determine the percolation largest component in interconnected networks. *Physical Review E*, 87(4):043302, 2013.
- [42] S Hwang, S Choi, Deokjae Lee, and B Kahng. Efficient algorithm to compute mutually connected components in interdependent networks. *Physical Review E*, 91(2):022814, 2015.
- [43] Florent Krzakala, Andrea Montanari, Federico Ricci-Tersenghi, Guilhem Semerjian, and Lenka Zdeborová. Gibbs states and the set of solutions of random constraint satisfaction problems. *Proceedings of the National Academy of Sciences*, 104(25):10318–10323, 2007.
- [44] Lenka Zdeborová and Florent Krzakala. Phase transitions in the coloring of random graphs. *Physical Review E*, 76(3):031131, 2007.
- [45] Guilhem Semerjian. On the freezing of variables in random constraint satisfaction problems. *Journal of Statistical Physics*, 130(2):251–293, 2008.
- [46] Flaviano Morone and Hernán A Makse. Influence maximization in complex networks through optimal percolation. *Nature*, 524(7563):65–68, 2015.
- [47] Alfredo Braunstein, Luca Dall’Asta, Guilhem Semerjian, and Lenka Zdeborová. Network dismantling. *Proceedings of the National Academy of Sciences*, 113(44):12368–12373, 2016.
- [48] Raffaele Marino, Giorgio Parisi, and Federico Ricci-Tersenghi. The backtracking survey propagation algorithm for solving random k-sat problems. *Nature communications*, 7(1):1–8, 2016.
- [49] Saeed Osat, Ali Faqeh, and Filippo Radicchi. Optimal percolation on multiplex networks. *Nature communications*, 8(1):1–7, 2017.
- [50] Valentina Ros, Gerard Ben Arous, Giulio Biroli, and Chiara Cammarota. Complex energy landscapes in spiked-tensor and simple glassy models: Ruggedness, arrangements of local minima, and phase transitions. *Physical Review X*, 9(1):011003, 2019.
- [51] Yanchen Liu, Nima Dehmamy, and Albert-László Barabási. Isotopy and energy of physical networks. *Nature Physics*, 17(2):216–222, 2021.
- [52] Laura Foini, Florent Krzakala, and Francesco Zamponi. On the relation between kinetically constrained models of glass dynamics and the random first-order transition theory. *Journal of Statistical Mechanics: Theory and Experiment*, 2012(06):P06013, 2012.
- [53] Pavel L Krapivsky, Sidney Redner, and Eli Ben-Naim. *A kinetic view of statistical physics*. Cambridge University Press, 2010.
- [54] Vincenzo Nicosia, Per Sebastian Skardal, Alex Arenas, and Vito Latora. Collective phenomena emerging from the interactions between dynamical processes in multiplex networks. *Physical review letters*, 118(13):138302, 2017.
- [55] A *feedback loop* condition is understood, i.e. if i in a is interdependent with j in b , and j in b is interdependent with k in c , then k and i are also interdependent.
- [56] Equivalent to cascading failures in interdependent percolation [6, 11, 37], where single networks reach first their equilibrium phases (percolation step) before propagating the damage (dependency step) to the dependent layers.
- [57] Negative values of the effective fields induce, additionally, an antiferromagnetic coupling (dashed lines in fig. 1, left box); these configurations are, nevertheless, transient and energetically disfavored.
- [58] Rajeev Motwani and Prabhakar Raghavan. *Randomized algorithms*. Cambridge university press, 1995.
- [59] Sidney Redner. *A guide to first-passage processes*. Cambridge university press, 2001.
- [60] W Klein, Harvey Gould, Natali Gulbahce, JB Rundle, and K Tiampo. Structure of fluctuations near mean-field critical points and spinodals and its implication for physical processes. *Physical Review E*, 75(3):031114, 2007.
- [61] Chris Unger and W Klein. Nucleation theory near the classical spinodal. *Physical Review B*, 29(5):2698, 1984.
- [62] K Binder. “clusters” in the ising model, metastable states and essential singularity. *Annals of physics*, 98(2):390–417, 1976.
- [63] DW Herrmann, W Klein, and D Stauffer. Spinodals in a long-range interaction system. *Physical Review Letters*, 49(17):1262, 1982.
- [64] W Klein and C Unger. Pseudospinodals, spinodals, and nucleation. *Physical Review B*, 28(1):445, 1983.
- [65] Florent Krzakala and Lenka Zdeborová. Hiding quiet solutions in random constraint satisfaction problems. *Physical review letters*, 102(23):238701, 2009.
- [66] Andrea Montanari, Federico Ricci-Tersenghi, and Guilhem Semerjian. Clusters of solutions and replica symmetry breaking in random k-satisfiability. *Journal of Statistical Mechanics: Theory and Experiment*, 2008(04):P04004, 2008.
- [67] Giorgio Parisi. On local equilibrium equations for clustering states. *arXiv preprint cs/0212047*, 2002.
- [68] Elegant connections. *Nature Physics*, 16:113, 2020.
- [69] Simon A Levin. The architecture of robustness. In *Global Challenges, Governance, and Complexity*. Edward Elgar Publishing, 2019.
- [70] Ling Sun, David Gerault, Adrien Benamira, and Thomas Peyrin. Neurogift: Using a machine learning based sat solver for cryptanalysis. In *International Symposium on Cyber Security Cryptography and Machine Learning*, pages 62–84. Springer, 2020.
- [71] Mária Ercsey-Ravasz and Zoltán Toroczkai. Optimization hardness as transient chaos in an analog approach to constraint satisfaction. *Nature Physics*, 7(12):966–970, 2011.
- [72] Marc Mézard and Andrea Montanari. Reconstruction on trees and spin glass transition. *Journal of statistical physics*, 124(6):1317–1350, 2006.
- [73] Yakov M Strel'niker, Richard Berkovits, Aviad Frydman, and Shlomo Havlin. Percolation transition in a two-dimensional system of ni granular ferromagnets. *Physical Review E*, 69(6):065105, 2004.
- [74] Alexander K Hartmann and Martin Weigt. *Phase transitions in combinatorial optimization problems*, volume 67. Wiley Online Library, 2005.
- [75] Marc Mézard and Giorgio Parisi. The bethe lattice spin glass revisited. *The European Physical Journal B-Condensed Matter and Complex Systems*, 20(2):217–233, 2001.
- [76] Giorgio Parisi, Pierfrancesco Urbani, and Francesco Zamponi. *Theory of simple glasses: exact solutions in infinite dimensions*. Cambridge University Press, 2020.
- [77] S. N. Dorogovtsev, A. V. Goltsev, and J. F. F. Mendes.

Critical phenomena in complex networks. *Rev. Mod. Phys.*, 80:1275–1335, Oct 2008.

- [78] Gourab Ghoshal, Vinko Zlatić, Guido Caldarelli, and Mark EJ Newman. Random hypergraphs and their applications. *Physical Review E*, 79(6):066118, 2009.
- [79] Owen T Courtney and Ginestra Bianconi. Generalized network structures: The configuration model and the canonical ensemble of simplicial complexes. *Physical Review E*, 93(6):062311, 2016.

METHODS

Partial interdependence. For partially interdependent Ising spin networks, Eq. (2) can be generalized to

$$-\mathcal{H}_{\mathcal{I}} = \sum_{i,j} \mathcal{A}_{ij} \sigma_i \sigma_j \left(\delta_{\sum_{\ell} \mathcal{I}_{i\ell}, 0} + \prod_{\ell} \mathcal{I}_{i\ell} \Sigma_{\ell} \right), \quad (7)$$

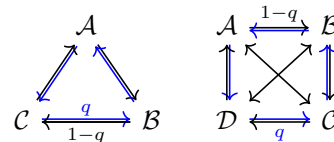
with $J \equiv 1$ for simplicity. In Eq. (7), the Kronecker delta sets pairwise links incoming in *independent* spins—i.e., indices $i = 1, \dots, MN$ satisfying the zero row sum condition $\sum_{\ell} \mathcal{I}_{i\ell} = 0$ —from their nearest neighbors.

For $M = 2$ networks with a fraction $q \in [0, 1]$ of one-to-one interdependent spins (e.g. the ER graphs studied in Fig. 3d), Eq. (7) simplifies to

$$-\mathcal{H}_{q,\mathcal{I}} = \sum_{\mu=A,B} \sum'_{i,j} A_{ij}^{\mu} \sigma_i^{\mu} \sigma_j^{\mu} + J \sum_{i,j,k} \mathcal{W}_{ijk} \sigma_i \sigma_j \sigma_k \quad (8)$$

where \sum' runs over the indices $i = 1, \dots, N$ of independent sites and the tensor \mathcal{W}_{ijk} is given by Eq. (3). Notice that Eq. (7) is, thus, a mixture of directed 2-spin and 3-spin interactions (as illustrated in Fig. 1).

For increasing number of layers, the degrees of freedom of the cross-layers couplings grow. E.g., for $M = 3$ networks, partial couplings can tune the system from 3 isolated layers to a mixture, like Eq. (9), of directed 2-spin and 4-spin couplings. Another option is a mixture of directed 3- and 4-spin interactions. In this case (i.e. results of Fig. 3c), one can consider a fraction q of *directed* interdependent links and a fraction $1 - q$ of one-to-one interdependent links (left diagram below).



Similar ideas can be applied at larger values of M e.g. to create mixtures of directed 4- and 5-spin interactions by coupling $M = 4$ layers (right diagram above).

Interdependent population dynamics. RS calculations (see SI) for isolated Ising ER graphs with average degree $\langle k \rangle$ yield the distributional equation

$$P(h) = e^{-\langle k \rangle} \sum_{k \in \mathbb{N}_0} \frac{\langle k \rangle^k}{k!} \int d\boldsymbol{\mu} \delta(h - \mathcal{T}_k(\beta; \mathbf{h})), \quad (9)$$

with integral measure $d\boldsymbol{\mu} \equiv \prod_{i=1}^k P(h_i) dh_i$ and kernel

$$\mathcal{T}_k(\beta; \mathbf{h}) \equiv \frac{1}{2\beta} \sum_{i=1}^k \log \left(\frac{f_+(\beta; h_i)}{f_-(\beta; h_i)} \right), \quad (10)$$

where $f_{\pm}(\beta; \chi) = \cosh(\beta(\chi \pm 1))$. Eq. (9) can be solved self-consistently for the distribution $P(h)$ of cavity fields $\{h_i\}_{i=1, \dots, N}$ via population dynamics methods [74]. For large enough populations (i.e. $N \sim 10^4 - 10^5$) and number of iterations (i.e. $T_{eq} \sim 10^3 - 10^4$), this yields also the

statistics of the (thermally averaged) local effective fields $\langle \Sigma_i \rangle_{\beta} = \sum_j A_{ij} \langle \sigma_j \rangle_{\beta} / k_i$, since the spins' magnetization is related to their cavities by $\langle \sigma_i \rangle_{\beta} = \tanh(\beta h_i)$.

In light of Eq. (1), we can then solve iteratively the sequence in Eq. (4) as follows. At each equilibrium stage (see Fig. 2a) we calculate the RS-cavity fields \mathbf{h}^{μ} of the μ -th network [75, 76] w.r.t. the β -distribution generated by its dependent layers, and then we update the β 's of the latter ones as in Eq. (4). Concretely, for an interdependent pair of spins σ_i in A and $\sigma_{i'}$ in B , the above can be represented as a recursion of local temperatures

$$\begin{aligned} \beta_{i',B}^{(n)} &= \beta k_i^{-1} \sum_j \mathcal{A}_{ij} \tanh \left(\beta_{j,A}^{(n-1)} h_{j,A}^{(n-1)} \right), \\ \beta_{i,A}^{(n)} &= \beta k_{i'}^{-1} \sum_{j'} \mathcal{A}_{i'j'} \tanh \left(\beta_{j',B}^{(n)} h_{j',B}^{(n)} \right), \end{aligned} \quad (11)$$

where $n \in \mathbb{N}$ and $\beta_{i,A}^{(0)} \equiv \beta$ is the initial seed. More generally, for an arbitrary network of fully-interdependent Ising networks, the recursion Eq. (11) reads as

$$\beta_{i_{\mu},\mu}^{(n)} = \beta \prod_{\ell_{\nu}(i_{\mu})} \mathcal{I}_{i_{\mu}\ell_{\nu}} \langle \Sigma_{\ell_{\nu}} \rangle_{\beta_{\nu}^{(n-1)}} \quad (12)$$

As $n \rightarrow \infty$, the β -distributions converge to configurations of local temperatures at which the layers' average magnetization $\{\mathcal{M}_{\infty}^{\mu}\}_{\mu=1,\dots,M}$ are mutually stable.

Given the above procedures, we have developed the interdependent population dynamics (iPD) algorithm summarized in the following pseudocode.

INTERPOPDYN($\beta, M, N, \mathcal{A}, \mathcal{I}, T_{eq}, NOI$)

```

1: Initialize the tensor  $\mathcal{W}_{i_1,\dots,i_M}$  from  $\mathcal{A}, \mathcal{I}$  as in Eq. (3);
2: Randomly initialize  $M$  populations  $\{\mathbf{h}^{\mu}\}_{\mu=1,\dots,M}$ ;
3: for  $n = 1, \dots, NOI$ : do
4:   for  $\mu = 1, \dots, M$ : do
5:     Compute  $\{\beta_{i_{\mu},\mu}^{(n)}\}_{i_{\mu}=1,\dots,N}$  as in Eq. (12);
6:   for  $t = 1, \dots, T_{eq}$ : do
7:     for  $i_{\mu} = 1, \dots, N$ : do
8:       Compute  $h_{i_{\mu}} = \mathcal{I}_{k_{i_{\mu}}}(\beta_{i_{\mu},\mu}^{(n)}, \{h_{j_{\mu}}\}_{j_{\mu} \in \partial i_{\mu}})$ ;
9:       Return the local fields  $\{\langle \Sigma_{i_{\mu}} \rangle_{\beta_{\mu}^{(n)}}\}_{i_{\mu}=1,\dots,N}$ ;
10: return array  $\{\mathcal{M}_{\infty}^{\mu}\}_{\mu=1,\dots,M}$ 

```

Since iPD builds on the *equilibrium* RS-solution of the diluted 2-spin model, $\mathcal{O}(MN)$ computational time can be saved by replacing the dependency steps (line 3) with the populations' equilibration (line 6). Partially interdependent systems are solved analogously, with the additional condition that the local temperature of independent spins stays T , i.e. the temperature of the heat bath.

Noisy-iPD runs alike the iPD above, with white noise added to the effective fields (line 9), i.e. by computing $\langle \Sigma_{i_{\mu}} \rangle_{\beta} + \xi_{i_{\mu}}$ with $\xi_{i_{\mu}} \in \mathcal{N}(0, a/(k)_{\mu})$. Finally, iPD with global OP interactions evolves analogously to the regular local iPD above, with Eq. (12) being replaced by

$$\beta_{i_{\mu},\mu}^{(n)} = \beta \prod_{\ell_{\nu}(i_{\mu})} \mathcal{I}_{i_{\mu}\ell_{\nu}} \mathcal{M}_{\nu}^{(n)}, \quad \mathcal{M}_{\nu}^{(n)} = \frac{1}{N} \sum_{i_{\nu}=1}^N \langle \Sigma_{i_{\nu}} \rangle_{\beta_{\nu}^{(n-1)}}.$$

Random XOR-SAT in a nutshell. Random K -XOR-SAT [36] searches for assignments to a Boolean vector $\mathbf{x} \in \{0, 1\}^N$ satisfying $\mathcal{C}\mathbf{x} = \mathbf{b} \pmod{2}$, where $\mathbf{b} \in \{0, 1\}^L$ is randomly given and \mathcal{C} is an $L \times N$ matrix underlying the structure of the $L = \alpha N$ randomly chosen K -tuple logical constraints. For $K = 3$, e.g., this corresponds to finding solutions to $F = \bigwedge_{\{i,j,k\} \in \mathcal{E}_3} x_i \oplus x_j \oplus x_k$, where \oplus is the XOR operation and the AND sum, \bigwedge , runs over all the triples $\{i, j, k\}$ in the edge list \mathcal{E}_3 of a random hypergraph. Through the mapping $\sigma_i = (-1)^{x_i}$ [31], K -XOR-SAT can be studied as the $T = 0$ limit of the diluted K -spin model $\mathcal{H} = \sum_{\{i_1, \dots, i_K\} \in \mathcal{E}_K} (1 - \sigma_{i_1} \cdots \sigma_{i_K})$. Similarly, random $(M+q)$ -XOR-SAT with $M = K-1$, i.e. a mixture of qL K -tuples and $(1-q)L$ M -tuples, can be solved by studying the $T = 0$ limit of a diluted $(M+q)$ -spin model.

Within the RS-ansatz (see SI for details), the complexity of random $(M+q)$ -XOR-SAT can be fully characterized via the zero-temperature free-energy density of a diluted $(M+q)$ -spin Hamiltonian, whose expression is

$$\begin{aligned} -\mathcal{F}/\ln 2 &= \phi(1 - \ln \phi) + \\ &- \frac{\langle k \rangle}{M+1} q [1 - (1 - \phi)^{M+1}] + \\ &- \frac{\langle k \rangle}{M} (1 - q) [1 - (1 - \phi)^M] \end{aligned} \quad (13)$$

where $\langle k \rangle \equiv K\alpha$ is the mean degree of the underlying hypergraph. Eq. (13) generalizes Eq. (5) (and other formulas discussed therein) to an arbitrary number M of ER graphs with the same average degree $\langle k \rangle$.

Asymptotics of M -DEP at large M . For $q = 1$, the branching OP for M interdependent ER graphs with average degree $\langle k \rangle$ minimizes Eq. (13) yielding the equation $m = \mathcal{G}(\langle k \rangle, m)$ with $\mathcal{G}(x, y) = 1 - \exp\{-xy^M\}$. At the spinodal $\partial_m \mathcal{G}|_{(\langle k \rangle_{sp}, m_{sp})} = 1$, leading to the closed formula $1/M = -(1 - m_{sp}) \ln(1 - m_{sp})/m_{sp}$. The latter yields an expansion for $m_{sp}(M)$ that, once inserted into $m_{sp} = \mathcal{G}(\langle k \rangle_{sp}, m_{sp})$ gives [45] $\langle k \rangle_{sp} = \ln K + \ln \ln K + 1 + \mathcal{O}(\ln \ln K / \ln K)$ with $K = M - 1$.

The asymptotics of the VUL-ROB threshold, $\langle k \rangle_{cx}(M)$, can be found instead by studying the zeroes of the configurational entropy (i.e. the K -XOR-SAT complexity)

$$\begin{aligned} \Sigma/\ln 2 &= m [1 + \langle k \rangle (1 - m)^M] + \\ &- \frac{\langle k \rangle}{M+1} [1 - (1 - m)^{M+1}], \end{aligned} \quad (14)$$

with $m = \mathcal{G}(\langle k \rangle, m)$. Since $(1 - m)^{M+1} \rightarrow 0$ and $\phi \rightarrow 1$ for $M \gg 1$, the null condition $\Sigma|_{(\langle k \rangle_{cx}, m_{cx})} = 0$ leads to $\langle k \rangle_{cx} \sim M + 1$. It follows that the metastability width has scaling $\langle k \rangle_{cx} - \langle k \rangle_{sp} \sim M - 1$ for $M \gg 1$, i.e. interdependent networks become less and less structurally stable as the number of interacting layers grows.

Annealed network approximation. For dense structures, the mapping revealed by the iPD between M randomly interdependent Ising networks and diluted K -spin models (Fig. 3a,b) can be verified analytically within the annealed network approximation [77]. Let us recall

that, given a typical ER graph $G \in \mathfrak{G}(N, p)$ with adjacency matrix $A = (A_{ij})_{i,j=1,\dots,N}$, the associated matrix of wiring probabilities has entries $\pi_{ij} := \langle A_{ij} \rangle_{\mathfrak{G}} \simeq \langle k \rangle / N$, where $\langle \dots \rangle_{\mathfrak{G}}$ is the average over the graph ensemble. Similarly, for configurational model networks, one finds $\pi_{ij} \simeq k_i k_j / \langle k \rangle N$. The annealed network approximation sums up to averaging over \mathfrak{G} the Hamiltonian, s.t. $A_{ij} \xrightarrow{a.a.} \pi_{ij}$. To apply the above to Eq. (2) we must, therefore, average over all the graph ensembles from where the networks composing the multilayer system are extracted. For one-to-one interdependence, this operation is straightforward due to trivial disorder governing the cross-layers pairings. In light of Eq. (3), the integration of interdependent interactions within the multilayer's structure yields the wiring tensor

$$\begin{aligned} \pi_{i_1 \dots i_K} &= \left\langle \dots \langle \mathcal{W}_{i_1 \dots i_K} \rangle_{\mathfrak{G}_K} \dots \right\rangle_{\mathfrak{G}_1} \\ &= \langle \mathcal{A}_{i_1 i_2} \rangle_{\mathfrak{G}_1} \prod_{\mu=1}^{M-1} \frac{\langle \mathcal{A}_{\ell_{\mu}(i_1) i_{\mu+2}} \rangle_{\mathfrak{G}_{\mu}}}{k_{\ell_{\mu}(i_1)}} \\ &= \frac{k_{i_1} k_{i_2}}{\langle k \rangle_1 N} \prod_{\mu=1}^{M-1} \frac{k_{i_{\mu+2}}}{\langle k \rangle_{\mu} N} \simeq \frac{k_{i_1} \dots k_{i_{M+1}}}{\langle k \rangle_1 \dots \langle k \rangle_M N^M}, \end{aligned}$$

with $K \equiv M + 1$, i.e. the wiring probability of an hypergraph in $d = M$ dimensions within the generalized configurational model [78, 79]. For ER graphs with equal average degree $\langle k \rangle$, analogous arguments yield $\pi \simeq \langle k \rangle / N^M$. One can then solve the Hamiltonian, Eq. (2), within the traditional Bragg-Williams approach, leading e.g. to the average magnetization $\mathcal{M} = \tanh(\beta \langle k \rangle \mathcal{M}^M)$ from where the (bulk) melting spinodals shown by arrows in Fig. 3a,b for $M = 2, 3$ can be readily calculated.

Contrarily with the above, partially-coupled networks break down the mapping. In the inset to Fig. 3c we supported this property via iPD numerics on ER graphs with finite connectivities, revealing an inversion in the difference of the (bulk) melting spinodals of the two models for increasing values of $\langle k \rangle$. In the annealed approximation, the differences between the two models become manifest. E.g. for $M = 2$ partially interdependent ER graphs and for a diluted $(2 + q)$ -spin model, one finds

$$\begin{aligned} \mathcal{M} &= q \tanh(\beta \langle k \rangle \mathcal{M}^2) + (1 - q) \tanh(\beta \langle k \rangle \mathcal{M}), \\ \mathcal{M} &= \tanh(\beta \langle k \rangle \mathcal{M} (1 - q(1 - \mathcal{M}))), \end{aligned}$$

respectively. Notice that the mapping holds for any $\langle k \rangle$ and for any M (see Fig. 3c, inset) when $q = 1$.

The annealed approximation provides only a coarse-grained view of the integrated structure underlying the interdependent Hamiltonian, Eq. (2). In fact, it neglects some essential microscopic details, such as the *actual* density of the higher-order interactions. Because of Eq. (1), the hypergraph integrating M fully-coupled ER graphs with average degrees $\{\langle k \rangle_{\mu}\}_{\mu=1,\dots,M}$ has, by construction, an average hyperedge density $\gamma_M = \prod_{\mu} \langle k \rangle_{\mu}$. Besides being directed, these hyperedges are also suitably weighted, s.t. a spin i_{μ} in the μ -th layer has, on average, γ_M incoming K -tuples with an average weight $\prod_{\nu \neq \mu} \langle k \rangle_{\nu}$. Hence i_{μ} sees, effectively, an average number $\langle k \rangle_{\mu}$ of incoming K -tuples, i.e. the same average degree of its own layer. While these microscopic details are negligible when heating up the system from its ferromagnetic phase, they become highly relevant when annealing it from its paramagnetic phase at low cooling rates. In this case, in fact, interdependent spin networks remain trapped in a supercooled malfunctioning (i.e. paramagnetic) phase, without undergoing the spin-glass transition expected in their ferromagnetic multi-spin analogue [32]. This is best shown in the inset of Fig. 3b for $M = 2$ and $q = 1$, where the spin-glass (SG) transition (indeed, its Kauzmann temperature) is marked by an arrow, whereas no similar threshold is observed in the interdependent spin model.

Data availability

Source codes can be freely accessed at the GitHub repository: https://github.com/BnayaGross/High_order_interdependent_ising. All other data that support the findings of this study are available from the corresponding author upon reasonable request.

Acknowledgments

I.B. warmly thanks W. Klein, H. Gould, S. Kirkpatrick, Y. Moreno, F. Radicchi and A. Frydman for fruitful comments and stimulating discussions. S.H. acknowledges financial support from the ISF, the China-Israel SF, the ONR, the BIU Center for Research in Applied Cryptography and Cyber Security, the EU project RISE, the NSF-BSF Grant No. 2019740, and the DTRA Grant No. HDTRA-1-19-1-0016.

Author contributions

I.B. initiated the work and designed the research, with contributions from B.G.. I.B. developed the algorithms and carried out the numerical and theoretical analyses. B.G. designed the codes and carried out the Monte Carlo simulations. S.H. supervised the research. I.B. wrote the paper with contributions from B.G. and S.H.. All authors critically reviewed and approved the manuscript.